Hindawi Publishing Corporation
International Journal of Antennas and Propagation
Volume 2011, Article ID 184942, 7 pages
doi:10.1155/2011/184942

Application Article

Dielectric Resonator Direction Finding Antenna

Laila Hady Salman,[1] Darko Kajfez,[1] and Ahmed A. Kishk[1,2]

[1] *Department of Electrical Engineering, The University of Mississippi, MS 38677, USA*
[2] *Department of Electrical and Computer Engineering, Concordia University, Montreal, QC, Canada H3G 1M8*

Correspondence should be addressed to Ahmed A. Kishk, kishk@encs.concordia.ca

Received 3 June 2011; Revised 9 September 2011; Accepted 13 September 2011

Academic Editor: Tayeb A. Denidni

The idea of using a cylindrical dielectric resonator antenna for mechanical direction finding and target tracking is presented. The hybrid feeding network of the receiving antenna comprised two ports: one for the broadside-type sum pattern and another for the monopole-type difference pattern. The proposed design is fabricated and tested experimentally for concept validation. Both linearly polarized patterns were obtained around 2.6 GHz. The coupling between the sum and difference ports is measured to be smaller than −30 dB, and the 3 dB width of the minimum in the difference pattern is 10°.

1. Introduction

Dielectric resonator antennas (DRAs) are alternative solutions to other conventional antenna types and preferable for wireless system applications due to their advantageous characteristics such as their small size, high radiation efficiency, wide impedance bandwidth, and low ohmic loss [1–6]. Recently, intensive research work has demonstrated the possibility of realizing multifunctional devices using single dielectric resonator through exciting multi-independent modes simultaneously. Such realizations were used for filtering, oscillating, packaging and radiating purposes [7–10]. This paper reports on the dual use of the single DRA, operating in the sum and difference mode, as reported in [11].

Traditionally, mechanical direction finding antennas were built with either loop or dipole antenna elements [12]. In radar applications, spiral and horn antennas have been used for the precision direction finding [13]. An alternative design which uses a single DRA for mechanical direction finding is proposed here. The operation is achieved by comparing the received signals of two DRA patterns. Those patterns are obtained by exciting $HEM_{11\delta}$ mode by two T-shaped patches, once out of phase and once in phase, to produce a broadside type and a monopole type of radiation patterns. Because of its small size, the proposed DRA can be used for an approximate hand-held target finding, but it could also be used as a feed for reflector antenna for an accurate direction finding in point-to-point applications.

Section 2 below provides a brief description of the proposed design configuration and the used design procedure. In Section 3, simulated results are compared with the measured results. The appendix provides the analysis of the hybrid feeding network for the antenna.

2. Proposed Design Geometry

The proposed design geometry is sketched in Figure 1, where the bottom view is shown for better understanding of the design configuration. It consists of a cylindrical dielectric resonator of 36.6 dielectric constant, 13.27 mm radius, and 8.33 mm height placed on top of a two-layer substrate with back-to-back ground plane alignment. To excite the resonator's hybrid $HEM_{11\delta}$ mode at two different ports simultaneously, a printed microstrip feeding network is placed on the bottom substrate layer of 10.2 dielectric constant and 0.625 mm thickness while coupled to the resonator through two T-shaped patches placed underneath the resonator and connected to the feeding network through conducting "vias" as shown in Figure 1. Wilkinson power dividers are used to provide the needed isolation between

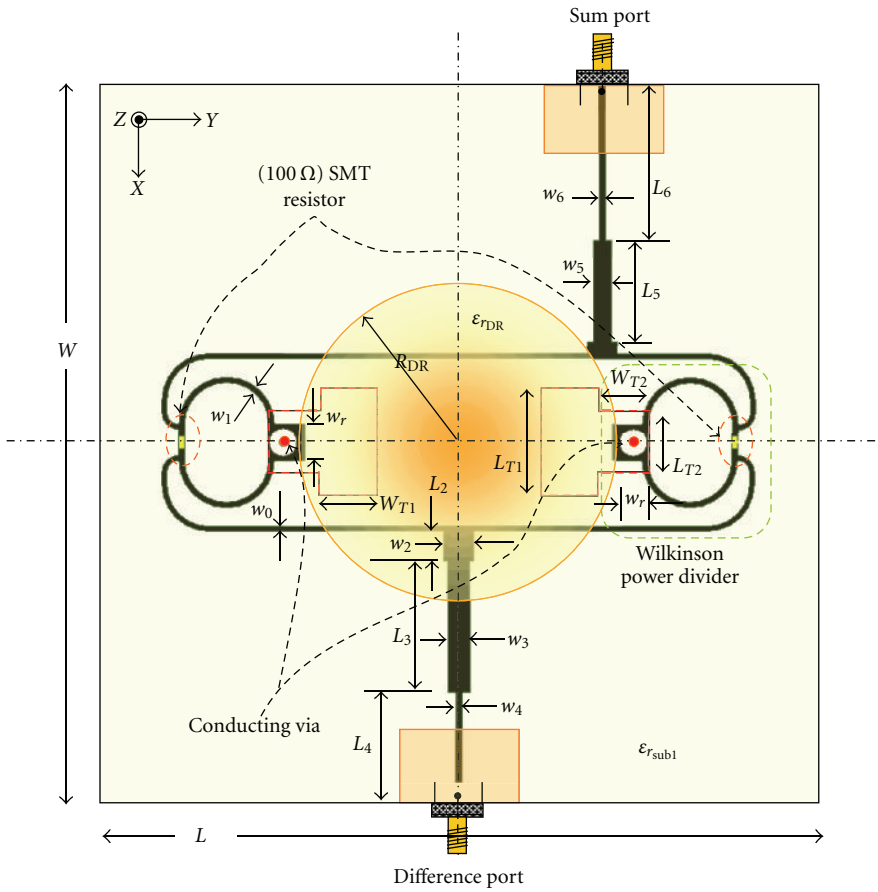

FIGURE 1: Top view of the proposed direction-finding geometry, where the bottom layer microstrip feeding network is shown in solid line.

the two ports. It is clear that this also added losses as described in the Appendix. The photographs of the front and back sides are shown in Figure 2.

The direction finding system is based on the sum and difference concept. It will be easier to explain the sum and difference radiation patterns in the transmitting mode of operation. Because of the reciprocity, the antenna pattern is the same whether the antenna is used in the receiving or the transmitting mode of operation. When the power is applied to the sum port, shown on top of Figure 1, the two vias excite the dielectric resonator in opposition of phase and with equal amplitudes, because the top left microstrip line is one half-wavelength longer than the top right microstrip line. With the use of the electromagnetic simulation package HFSS [14], it is possible to plot the resulting electric field distribution for such excitation of the dielectric resonator. Figure 3(a) shows the electric field at the upper face of the dielectric resonator. It is seen that most of the electric field inside and outside of the resonator is horizontally oriented. Such a field distribution will produce a horizontally polarized far field, which will have maximum radiation in the broadside direction. For that reason, the antenna port at the top of Figure 1 is called the sum port.

On the other hand, when the power is applied to the bottom port in Figure 1, the two vias that excite the dielectric resonator are fed with equal phase and equal magnitude, because the microstrip lines leading to the vias are of an equal length. The electric field distribution for such an excitation is plotted in Figure 3(b). It is observed that most of the field vectors oppose each other for a radiation in the broadside radiation. In particular, the field outside the resonator is strong and mostly oriented in radial direction, as if produced by a monopole in place of the dielectric resonator. For that reason, the lower port of the structure in Figure 1 is called the difference port. As the field lines are radial and orthogonal to the dielectric surface, their strength just outside the dielectric is stronger than the radial components just inside by the value of the dielectric constant.

The structure consists of two microstrip substrates with the common grounds touching each other. The top layer substrate has 2.94 dielectric constant and 1.524 mm thickness so that the $HEM_{11\delta}$ mode is expected to resonate around 2.4 GHz. The bottom layer feeding network is shown as solid lines in Figure 1 while the upper layer T-shaped patches are in dashed lines. The proposed microstrip line feeding network for the $HEM_{11\delta}$ mode excitation is printed on the bottom face of the discussed module. The design was simulated using HFSS design software [14]. To allow the $HEM_{11\delta}$ mode coupling with the dielectric resonator, two T-shaped patches are placed underneath the dielectric

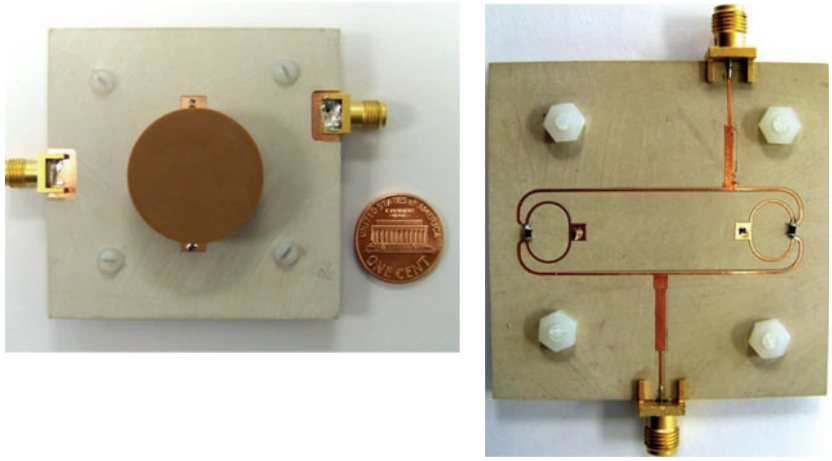

(a) (b)

Figure 2: Physical layout of the proposed direction-finding antenna (a) top view, (b) bottom view.

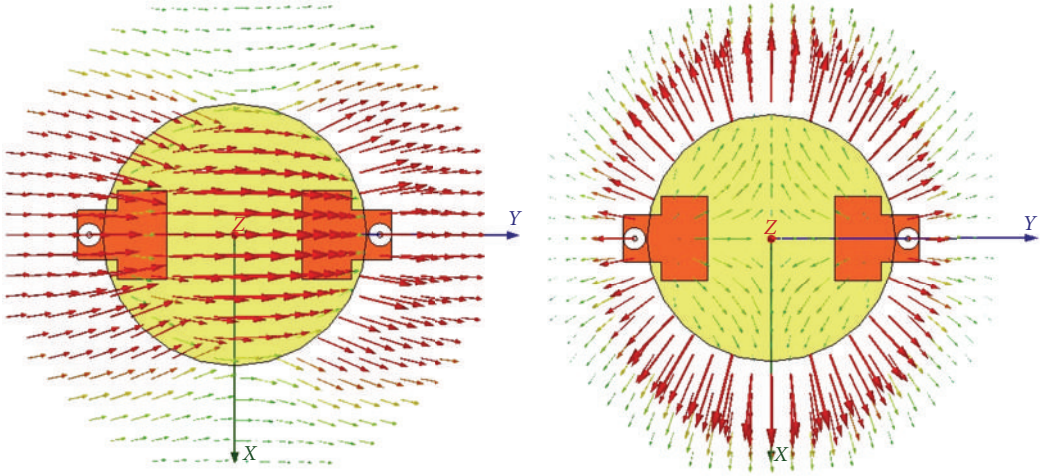

(a) (b)

Figure 3: (a): Electric field distribution when the power is applied to the sum port and (b): the power is applied to the difference port. The two T-shaped patches are connected to the bottom microstrip network by vias.

resonator while connected to the bottom face microstrip circuit by conducting "vias" as shown in Figure 4.

To achieve sum and difference ports matching and acceptable isolation between them, Wilkinson power dividers are used [15]. Simulated and measured results at the output ports, illustrated in Figure 5, demonstrate that an isolation of more than 30 dB between the sum and difference ports was achieved, while both ports are matched to better than −10 dB around the frequency of 2.6 GHz.

As shown in the Appendix, if the sum port is excited, the two vias will be equal in magnitude and out of phase and if the difference port is excited, the two vias will be equal in magnitude and in phase.

3. Measured and Simulated Results

The proposed geometry from Figure 1 was built and measured to verify the computed results. The physical layout of the proposed structure is in Figure 2, where the top view is shown in Figure 2(a) after attaching the resonator on top of the T-shaped patches. On the other hand, the microstrip feeding network is observed in Figure 2(b) for completeness.

The original design was intended to work around 2.4 GHz which makes it applicable for WLAN applications. The measurements on the fabricated design showed the operating frequency to be centered at 2.6 GHz. A disagreement was probably caused by machining inaccuracies and by the existence of an air gap under the resonator. Table 1 lists all the design parameters that are used in the above figures.

After the simulated results were scaled to frequency 2.6 GHz, one can observe an acceptable agreement with the measured results, as shown in Figure 5. The isolation between the difference and sum ports is in the range of 30 dB within the bandwidth of interest.

Far field radiation patterns were also measured to verify the suitability of the antenna for the direction-finding

Table 1: Design parameters of the proposed direction-finding structure using dielectric resonator.

Parameter Symbol	Parameter Value (mm)	Parameter Symbol	Parameter Value (mm)
L	60	W_{T2}	4
W	60	w_r	3
w_0	0.55	L_2	2.5
w_1	0.35	L_3	11
w_2	2.5	L_4	8.5
w_3	1.82	L_5	8.4
w_4	0.55	L_6	11
w_5	1.5	L_{T1}	9
w_6	0.55	L_{T2}	5
W_{T1}	5		

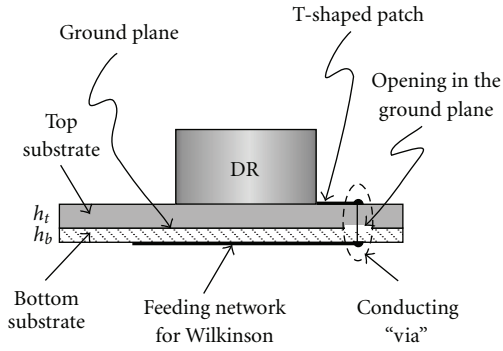

Figure 4: Side view of the proposed DRA structure.

purposes. Both sum and difference radiation patterns were measured and compared with the simulated results as shown in Figures 6 and 7, respectively.

A monopole type of radiation patterns were observed in both XZ and YZ planes when exciting the difference port while terminating the sum port with matched load as shown in Figure 6. The measured cross-polarization level is at least 17 dB below the copolar level as predicted by the simulations. Broadside type patterns were obtained when exciting the sum port while terminating the difference port with matched load, as shown in Figure 7. A cross-polar level is measured to be at least 22 dB below the copolar level.

We did not measure the gain of the antenna, but we computed the directivity with the HFSS software [14]. In the broadside direction, the directivity of the sum radiation pattern is 6.3 dB, and the directivity of the difference radiation pattern in the same direction is −22.2 dB. Therefore, the cross coupling of −30 dB, measured in Figure 5, is sufficiently small for a reliable detection of the minimum. From the measured radiation pattern in Figure 6(b), we estimate that one can expect the resolution of the tracking operation in the YZ plane to be ±5° or better.

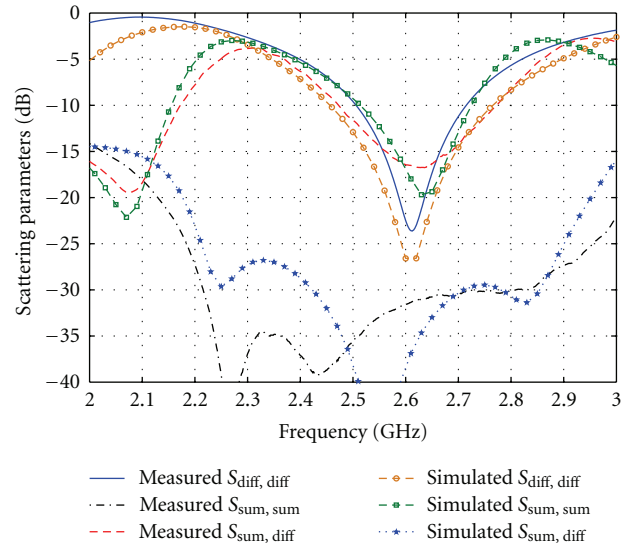

Figure 5: Measured and simulated scattering parameters.

4. Conclusion

The concept of using a cylindrical dielectric resonator to implement a direction-finding antenna system has been designed, fabricated, and tested. Both monopole-type and broadside-type of radiation patterns were observed when the dielectric resonator was excited at two different ports. The dielectric resonator antenna operates around $HEM_{11\delta}$ mode resonance, which creates linearly polarized far field patterns. Simulated and measured results were carried out to prove that such a configuration can be applied in direction-finding systems. The intended application of this antenna is to locate a position of a source of radiation. Because of its small size, it can be hand-held, for instance, to locate the position of a parked car in the parking space of a football stadium. With minor dimension modifications, the structure can be made suitable for the WLAN applications.

Appendix

Hybrid Feed Network Analysis

The diagram of the hybrid feed network is shown in Figure 8. The characteristic impedances of all the interconnecting microstrip transmission lines are equal to 50 Ω. The sum port S, shown on top of the diagram, is normalized to 25 Ω, and the difference port D, shown on the bottom, is likewise normalized to 25 Ω for simplicity of analysis. As shown in Figure 1, the input impedances of the sum and difference ports are later transformed with quarter-wave transformers back to 50 Ω, but this is of no importance for the analysis described below. The T-junctions between the 50 Ω and 25 Ω lines are denoted by letter J, and the Wilkinson power dividers [15] are denoted by letter W. The two ports which are to be connected to the dielectric resonator antenna by vias are denoted as left port L and right port R.

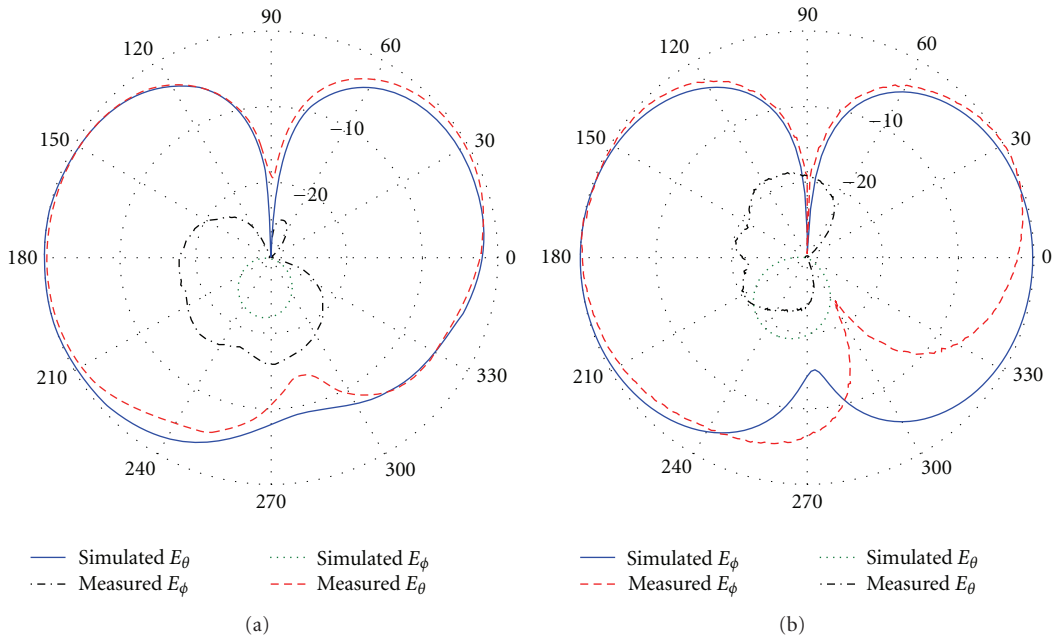

FIGURE 6: Comparison between simulated and measured radiation patterns for the $HEM_{11\delta}$ mode at 2.6 GHz when the difference mode is activated (a) XZ plane (b) YZ plane, in dB units.

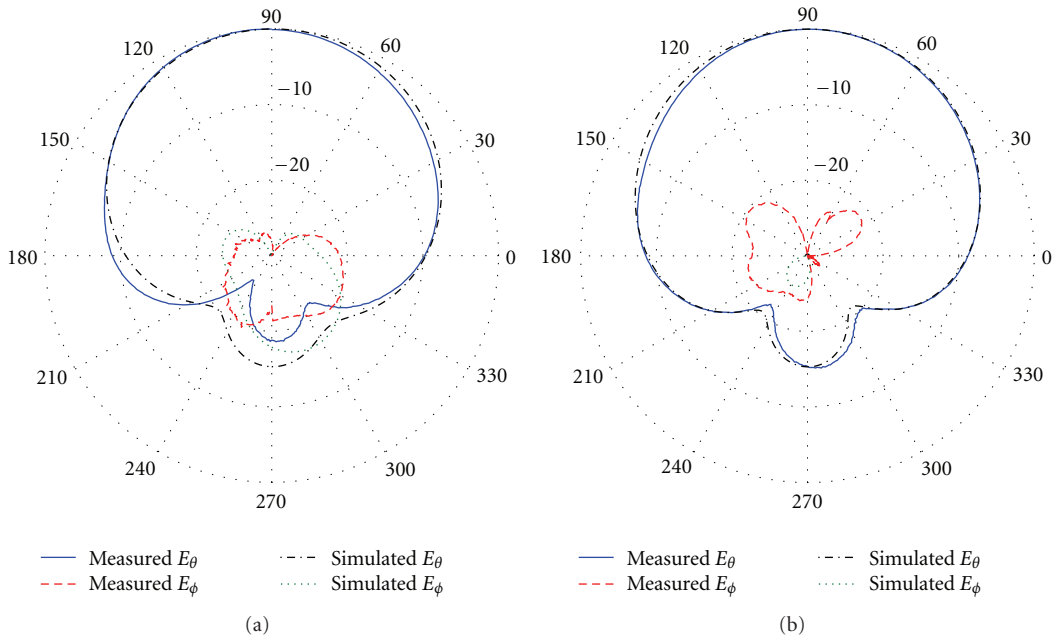

FIGURE 7: Simulated and measured radiation patterns for the $HEM_{11\delta}$ mode at 2.6 GHz when the sum mode is activated (a) XZ plane (b) YZ plane, in dB units.

The phase lengths of the interconnecting transmission lines are denoted θ_1 to θ_4. For the network at hand, the phase lengths have been selected as follows:

$$\theta_1 = \frac{3\pi}{2}; \quad \theta_2 = \pi; \quad \theta_3 = \frac{\pi}{2}; \quad \theta_4 = \pi. \tag{A.1}$$

Note that the hybrid feed network differs from the traditional hybrid ring [16] because the total circumference of the former is 2 wavelengths, while the circumference of the latter is only 1.5 wavelengths.

It is convenient to display the overall scattering matrix of the entire network in a partitioned form. For this purpose,

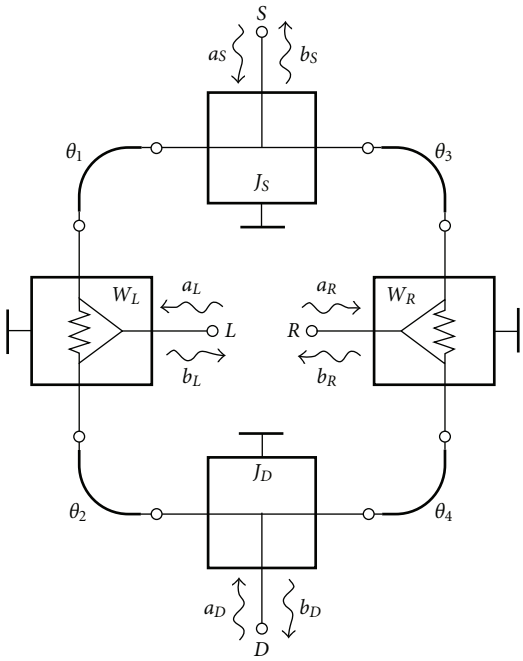

Figure 8: Diagram of the feeding network for the direction finding antenna.

define the column vectors for outgoing and incoming waves at antenna ports

$$|b_1\rangle = \begin{pmatrix} b_L \\ b_R \end{pmatrix}; \quad |a_1\rangle = \begin{pmatrix} a_L \\ a_R \end{pmatrix}. \tag{A.2}$$

Similarly, the outgoing and incoming wave vectors at feeding ports are

$$|b_2\rangle = \begin{pmatrix} b_S \\ b_D \end{pmatrix}; \quad |a_2\rangle = \begin{pmatrix} a_S \\ a_D \end{pmatrix}. \tag{A.3}$$

The overall scattering matrix of the feed network is then described in partitioned form by

$$|b_1\rangle = \mathbf{S}_{11}|a_1\rangle + \mathbf{S}_{12}|a_2\rangle, \tag{A.4}$$

$$|b_2\rangle = \mathbf{S}_{21}|a_1\rangle + \mathbf{S}_{22}|a_2\rangle, \tag{A.5}$$

where $\mathbf{S}_{ij}$ are 2×2 matrices. When the phase lengths from (A.3) are used, the corresponding matrices come out to be

$$\mathbf{S}_{11} = \frac{1}{2}\begin{pmatrix} 0 & -1 \\ -1 & 0 \end{pmatrix}, \tag{A.6}$$

$$\mathbf{S}_{12} = \frac{1}{2}\begin{pmatrix} 1 & j \\ -1 & j \end{pmatrix}, \tag{A.7}$$

$$\mathbf{S}_{21} = \frac{1}{2}\begin{pmatrix} 1 & -1 \\ j & j \end{pmatrix}, \tag{A.8}$$

$$\mathbf{S}_{22} = \begin{pmatrix} 0 & 0 \\ 0 & 0 \end{pmatrix}. \tag{A.9}$$

Suppose that an incoming wave a_s is applied to port S, and the remaining three ports are terminated in the matched loads (i.e., $a_L = a_R = a_D = 0$). From (A.4), it follows that

$$b_L = \frac{1}{2}a_S; \quad b_R = -\frac{1}{2}a_S. \tag{A.10}$$

Thus, the signal coming out of port L is in opposition of phase with the signal coming out of port R, as required for the maximum radiation in the broadside direction. Unfortunately, the sum of powers coming out of port L and port R is only one-half of the power entering the port S. The other half of the incoming power is dissipated in Wilkinson's power dividers. In a similar way, it is found that when the power is applied to port D, while the other three ports are terminated in matched loads, the ports L and R are excited with equal amplitudes and equal phases, as required for the zero radiation in the broadside direction. Again, half of the power is lost inside Wilkinson's power dividers.

It can be seen from (A.5) and (A.9) that there is no cross coupling between port S and port D, when the antenna ports are terminated in matched loads. This happens because $\mathbf{S}_{22}$ is a zero matrix, thanks to Wilkinson's power dividers.

When the dielectric resonator antenna is inserted between ports L and R, the possibility arises for a cross coupling between ports S and D. The antenna is described by its scattering matrix $\mathbf{S}_A$

$$|a_1\rangle = \mathbf{S}_A|b_1\rangle. \tag{A.11}$$

The sizes of the coupling pads in Figure 4 have been designed for the input impedance to be close to the $50\,\Omega$ value. The remaining reflection coefficient, here denoted by g, is a complex number with absolute value considerably smaller than unity. The transmission coefficient of the antenna, here denoted by h, is also a complex number with an absolute value smaller than unity. Thus, the antenna scattering matrix is of the form

$$\mathbf{S}_A = \begin{pmatrix} g & h \\ h & g \end{pmatrix}. \tag{A.12}$$

To evaluate the amount of the cross coupling, (A.12) is used to eliminate $|a_1\rangle$ and $|b_1\rangle$from (A.4) and (A.5). The resulting two-port between ports S and D is then described by [17, p. 251]

$$|b_2\rangle = \left[\mathbf{S}_{22} + \mathbf{S}_{21}\mathbf{S}_A(1 - \mathbf{S}_{11}\mathbf{S}_A)^{-1}\mathbf{S}_{12}\right]|a_2\rangle = \mathbf{S}_T|a_2\rangle. \tag{A.13}$$

Since h and g are small, the inverse matrix operation appearing in (A.13) can be approximated as follows:

$$(1 - \mathbf{S}_{11}\mathbf{S}_A)^{-1} \cong 1 + \mathbf{S}_{11}\mathbf{S}_A + \mathbf{S}_{11}\mathbf{S}_A\mathbf{S}_{11}\mathbf{S}_A + \cdots. \tag{A.14}$$

Thus, the first three terms of the matrix $\mathbf{S}_T$ are:

$$\mathbf{S}_T = \mathbf{S}_{21}\mathbf{S}_A\mathbf{S}_{12} + \mathbf{S}_{21}\mathbf{S}_A\mathbf{S}_{11}\mathbf{S}_A\mathbf{S}_{12} + \mathbf{S}_{21}\mathbf{S}_A\mathbf{S}_{11}\mathbf{S}_A\mathbf{S}_{11}\mathbf{S}_A\mathbf{S}_{12}. \tag{A.15}$$

After performing the matrix multiplications in (A.15), it is found that the off-diagonal terms are zero. Therefore, port S is decoupled from the port D, as long as the antenna is passive and reciprocal, and it is built in a symmetrical fashion so that its impedance matrix has a form such as in (A.12). On the other hand, the terms on the main diagonal of the matrix $\mathbf{S}_T$ are not zero. Because of that, the nonvanishing terms on the main diagonal of the matrix $\mathbf{S}_T$ indicate that the dielectric resonator antenna contributes to the mismatch seen at ports S and D.

Acknowledgments

This work was supported by the National Science Foundation under Grant no. ECS-524293. The authors would like to thank Trans-Tech Company for providing free samples of the dielectric resonator and Rogers Corporation for providing free laminate substrates.

References

[1] A. A. Kishk and A. Z. Elsherbeni, "Radiation characteristics of cylindrical dielectric resonator antennas with new applications," *IEEE Antennas and Propagation Society*, vol. 31, no. 1, pp. 7–16, 1989.

[2] D. Kajfez and P. Guillon, *Dielectric Resonators*, Noble Publishing, Atlanta, Ga, USA, 1998.

[3] S. H. Ong, A. A. Kishk, and A. W. Glisson, "Rod-ring dielectric resonator antenna," *International Journal of RF and Microwave Computer-Aided Engineering*, vol. 14, no. 5, pp. 441–446, 2004.

[4] A. A. Kishk, "Experimental study of broadband embedded dielectric resonator antennas excited by a narrow slot," *IEEE Antennas and Wireless Propagation Letters*, vol. 4, no. 1, pp. 79–81, 2005.

[5] A. A. Kishk, R. Chair, and K. F. Lee, "Broadband dielectric resonator antennas excited by L-shaped probe," *IEEE Transactions on Antennas and Propagation*, vol. 54, no. 8, pp. 2182–2189, 2006.

[6] R. Chair, A. A. Kishk, and K. F. Lee, "Low profile wideband embedded dielectric resonator," *IET Microwaves, Antennas and Propagation*, vol. 1, no. 2, pp. 294–298, 2007.

[7] E. H. Lim and K. W. Leung, "Novel utilization of the dielectric resonator antenna as an oscillator load," *IEEE Transactions on Antennas and Propagation*, vol. 55, no. 10, pp. 2686–2691, 2007.

[8] E. H. Lim and K. W. Leung, "Use of the dielectric resonator antenna as a filter element," *IEEE Transactions on Antennas and Propagation*, vol. 56, no. 1, pp. 5–10, 2008.

[9] L. K. Hady, D. Kajfez, and A. A. Kishk, "Dielectric resonator antenna in a polarization filtering cavity for dual function applications," *IEEE Transactions on Microwave Theory and Techniques*, vol. 56, no. 12, part 2, pp. 3079–3085, 2008.

[10] L. K. Hady, D. Kajfez, and A. A. Kishk, "Triple mode use of a single dielectric resonator," *IEEE Transactions on Antennas and Propagation*, vol. 57, no. 5, pp. 1328–1335, 2009.

[11] L. K. Hady, A. A. Kishk, and D. Kajfez, "Dielectric resonator antenna utilization as a direction finder," in *Proceedings of the IEEE International Symposium on Antennas and Propagation and USNC/URSI National Radio Science Meeting (APSURSI '09)*, pp. 1–4, June 2009.

[12] Y. T. Lo and S. W. Lee, *Antenna Handbook: Theory, Applications and Design*, D. Van Nostrand Reinhold Company, New York, NY, USA, 1988.

[13] S. E. Lipsky, *Microwave Passive Direction Finding*, SciTech Publishing, Raleigh, NC, USA, 2004.

[14] HFSS commercial software is distributed by Ansys. Inc., http://www.ansys.com.

[15] E. Wilkinson, "An N-way hybrid power divider," *IEEE Transactions on Microwave Theory and Techniques*, vol. 8, pp. 116–118, 1960.

[16] C. Y. Pon, "Hybrid-ring directional coupler for arbitrary power divisions," *IEEE Transactions on Microwave Theory and Techniques*, vol. 9, pp. 529–535, 1961.

[17] D. Kajfez, *Notes on Microwave Circuits*, vol. 1, Kajfez Consulting, Oxford, Miss, USA, 1984.